

1 **Short title:** Novel cytokinin–jasmonate crosstalk in maize.

2

3 ***Corresponding author:** Michael G. Muszynski: mgmuszyn@hawaii.edu

4

5 **Authors names and affiliations:** Aimee N. Uyehara^{1,a}, Angel R. Del Valle-Echevarria¹, Charles
6 T. Hunter², Hilde Nelissen^{3, 4}, Kirin Demuynck^{3, 4}, James F. Cahill^{5,b}, Georg Jander⁶, Michael G.
7 Muszynski^{1,*}

8

9 1. Department of Tropical Plant and Soil Sciences, University of Hawai'i at Mānoa,
10 Honolulu, HI, 96822, USA

11 2. Chemistry Research, Center for Medical, Agricultural and Veterinary Entomology,
12 USDA-ARS, Gainesville, FL, 32608, USA

13 3. Department of Plant Biotechnology and Bioinformatics, Ghent University, Gent, Belgium

14 4. Center for Plant Systems Biology, VIB, Gent, Belgium

15 5. Department of Genetics, Development and Cell Biology, Iowa State University, Ames,
16 Iowa, 50011

17 6. Boyce Thompson Institute for Plant Research, Cornell University, Ithaca, New York
18 14853

19

20 A. Present address: Department of Botany and Plant Sciences, University of California,
21 Riverside, CA 92521

22 B. Corteva AgrisciencesTM, Agriculture Division of DowDuPont, Johnston, IA 50131, USA

23

24

25 **Article Title:** Cytokinin promotes jasmonic acid accumulation in the control of maize leaf
26 growth.

27

28 **One sentence summary:**

29 Cytokinin-signaling upregulates the jasmonate biosynthesis pathway, resulting in jasmonate
30 accumulation and influences on maize leaf growth.

31

32

33

34

35 **Author contributions**

36 M.G.M. and A.R.D.V. designed the experiments, A.N.U., A.R.D.V., G.J., C.T.H., H.N., and
37 J.F.C. performed experiments and analyzed data, and A.N.U. wrote the paper with input from
38 other authors.

39

40 **Abstract**

41 Growth of plant organs results from the combined activity of cell division and cell expansion.
42 The coordination of these two processes depends on the interplay between multiple hormones
43 that determine final organ size. Using the semidominant *Hairy Sheath Frayed1 (Hsf1)* maize
44 mutant, that hypersignals the perception of cytokinin (CK), we show that CK can reduce leaf
45 size and growth rate by decreasing cell division. Linked to CK hypersignaling, the *Hsf1* mutant
46 has increased jasmonic acid (JA) content, a hormone that can inhibit cell division. Treatment of
47 wild type seedlings with exogenous JA reduces maize leaf size and growth rate, while JA
48 deficient maize mutants have increased leaf size and growth rate. Expression analysis revealed
49 increased transcript accumulation of several JA pathway genes in the *Hsf1* leaf growth zone. A
50 transient treatment of growing wild type maize shoots with exogenous CK also induced JA
51 pathway gene expression, although this effect was blocked by co-treatment with cycloheximide.
52 Together our results suggest that CK can promote JA accumulation possibly through increased
53 expression of specific JA pathway genes.

54

55

56

57 **INTRODUCTION**

58

59 Growing plants accumulate biomass over time through the integration of cell division and cell
60 expansion. These processes produce biomass by increasing cell number (cell division) and
61 increasing final cell volume (expansion). In eudicot leaves, the placement and timing of cell
62 division, expansion, and differentiation determines the pattern of leaf growth. In many model
63 plants, leaf growth follows a basipetal pattern where differentiation starts at the distal tip of the
64 leaf and finishes near the proximal base (Gupta and Nath, 2016; Conklin et al., 2019). Other
65 growth patterns include acropetal growth (differentiation starts at the proximal base), diffuse
66 growth (differentiation occurs evenly across the leaf without respect to cellular proximal-distal
67 position), and bidirectional growth (differentiation begins at both the distal tip and proximal base)
68 (Gupta and Nath, 2016).

69 Growth is controlled, in part, by signaling between plant hormones. Plant hormones are
70 molecular messengers with low molecular weights that regulate growth, development, and
71 defense (Santner and Estelle, 2009; Wolters and Jürgens, 2009; Frébort et al., 2011; Huot et
72 al., 2014). Generally, plant hormones can be divided into two classes: growth hormones and
73 defense hormones. Classical growth hormones include, cytokinin (CK), gibberellins (GA),
74 brassinosteroids (BR) and auxin (Huot et al., 2014). These hormones have been ascribed
75 functions in cell proliferation, stem elongation, seed germination, and organ elongation
76 respectively. Classical defense hormones include salicylic acid (SA), jasmonic acid (JA), and
77 ethylene (ET), and are responsible for the majority of signaling in response to pests and
78 pathogens (Huot et al., 2014). Coordination between growth and defense pathways is
79 necessary for appropriate allocation of resources in response to environmental stimuli, and is
80 mediated by hormone crosstalk. One described example of crosstalk is the signaling between
81 GA and JA. In the presence of JA, the GA repressor DELLA is released to bind and degrade GA
82 leading to suppression of GA-mediated growth by JA (Hou et al., 2013). In contrast, BR seems
83 to relieve JA-induced growth suppression, suggesting an antagonistic relationship between BR
84 and JA (Huot et al., 2014). Crosstalk has also been shown to occur between SA and auxin. SA
85 represses auxin-mediated growth by repressing the transcription of the F-box protein TIR1/AFB,
86 leading to the stabilization of the auxin repressor AUX/IAA (Wang et al., 2007; Huot et al.,
87 2014). As predicted by the growth-defense tradeoff model, signaling by defense hormones to
88 growth hormones often leads to growth suppression.

89 Growth of the maize leaf occurs at its base within zones of cell division and expansion
90 that are spatially distinct. The maize leaf contains multiple growth associated hormones which
91 crosstalk to regulate and define the leaf growth zones (Nelissen et al., 2012). The maize leaf
92 develops from the maize leaf initials on the shoot apical meristem. The leaf tip is formed first
93 and is propelled distally by proliferative divisions at the leaf base (Kiesselbach, 1999). In
94 monocot leaves, the basipetal growth mechanism sets up regions of division, elongation, and
95 maturation that are linearly organized and spatially separated into distinct growth zones
96 (Nelissen et al., 2016). The linear organization of the growth zones makes it straightforward to
97 use kinematic analysis to measure the relative contribution of division and expansion to final leaf
98 size (Nelissen et al., 2013). Kinematic analysis provides insight into the complex molecular
99 interactions underlying leaf growth as different hormones have measurable and distinct impacts
100 on the growth zones. This was demonstrated through kinematic analysis of GA biosynthesis
101 mutants in maize (Nelissen et al., 2012). It was shown that increased bioactive GA increases
102 the size of the division zone and determine the spatial location of the division-elongation

103 transition zone (Nelissen et al., 2012). These data also implicated other growth hormones such
104 as cytokinin, auxin, and brassinosteroids as possible players in determining the size of the
105 division zone (Nelissen et al., 2012).

106 Cytokinin (CK) is a growth promoting hormone that regulates processes such as shoot
107 growth, apical dominance, senescence, and promotion of cell proliferation (Miller et al., 1955;
108 Werner et al., 2001). In dicots, cytokinin promotes leaf growth by stimulating cell division. This
109 has been demonstrated through exogenous CK treatment, overexpression of CK catabolic
110 enzymes, or knockout of CK receptors. For example, decreasing endogenous CK concentration
111 through the overexpression of the CK catabolic enzyme, CYTOKININ OXIDASE (CKX) in
112 *Nicotiana tabacum* reduced leaf size by reducing cell number (Werner et al., 2001). In
113 *Arabidopsis thaliana*, reduction of CK signaling through the knockout of the CK receptor
114 *Arabidopsis* HISTIDINE KINASE 2 (AHK2), AHK3, and CRE1/AHK4 resulted in plants with
115 severely reduced rosette size and a reduced number of cells per leaf (Riefler et al., 2006).
116 Reduced cell number as a result of reduced cytokinin perception or signaling resulted in growth
117 compensation through cell expansion (Werner et al., 2001; Riefler et al., 2006). In contrast,
118 constitutively active CK receptor mutants in *A. thaliana* exhibited larger leaves with more
119 epidermal cells due to either an extended period of mitotic activity, increased mitotic rate, or
120 both (Bartrina et al., 2017).

121 The role of CK in regulating monocot leaf growth is less clear. In contrast to *Arabidopsis*,
122 maize has seven CHASE-domain histidine kinase receptors (Lomin et al., 2011; Steklov et al.,
123 2013). The maize mutant *Hairy Sheath Frayed1* (*Hsf1*) is the only CK receptor gain-of-function
124 monocot mutant. *Hsf1* is a semidominant mutant with an EMS-induced mutation in the cytokinin
125 receptor, *Zea mays* HISTIDINE KINASE1 (*ZmHK1*), an orthologue of *AtHK4* (Bertrand-Garcia
126 and Freeling, 1991; Muszynski et al., 2019). Characterization of *Hairy Sheath Frayed1* (*Hsf1*)
127 demonstrated the role of increased CK signaling had on leaf patterning, leaf size, and epidermal
128 cell fate (Bertrand-Garcia and Freeling, 1991; Muszynski et al., 2019). Although CK typically
129 promotes cell division and growth, increased signaling (hypersignaling) of CK in *Hsf1* mutants
130 reduced leaf growth compared to wild-type siblings (Muszynski et al., 2019). The effect of
131 reduced CK on monocot growth was indirectly observed through transgenic overexpression of
132 zeatin O-glucosylzeatin, an enzyme that inactivates and sequesters CK through the addition of
133 a sugar moiety (Pineda Rodo et al., 2008). Homozygous *Ubi:ZOG1* maize lines showed CK
134 deficiency phenotypes such as reduced growth and interestingly, a feminized tassel (Pineda
135 Rodo et al., 2008).

136 Jasmonic acid (JA) is an established plant growth regulator involved in processes such
137 as leaf senescence, plant defense, and male fertility (Yan et al., 2014). Linolenate lipoygenase
138 (LOX) catalyzes the first step of JA biosynthesis from chloroplast membrane phospholipids
139 (Lyons et al., 2013). The resulting hydroperoxy octadecadienoic acids are further converted into
140 (+)-7-iso-JA via allene oxide synthase (AOS), allene oxide cyclase (AOC), 12-oxophytodienoic
141 reductase (OPR) and three cycles of β -oxidation (Lyons et al., 2013). Bioactive JA-Ile is formed
142 through the conjugation of an amino acid by the jasmonate amido synthetase (JAR) (Lyons et
143 al., 2013). Catabolism of JA-Ile occurs through the oxidation of JA-Ile by the cytochrome
144 CYP94B enzyme (Lunde et al., 2019). Research on JA's role as both a defense and plant
145 growth regulator is aided by biosynthesis and signaling mutants. In maize, mutants for LOX,
146 OPR, and CYP94B include *tasselseed1*, *opr7-5 opr8-2*, and *Ts5* respectively (Acosta et al.,
147 2009; Yan et al., 2012; Lunde et al., 2019). These mutants add to a growing body of research
148 that establishes JA as a growth repressor. Initial studies showed that exogenous JA application
149 to rice seedlings reduced seedling leaf size (Yamane et al., 1980). More recently, wound
150 induction of JA and analysis of *Arabidopsis* JA biosynthesis mutants have shown that JA
151 suppresses cell proliferation leading to reduced leaf size with fewer and smaller epidermal cells
152 (Zhang and Turner, 2008; Noir et al., 2013).

153 Here, we show that CK signaling reduces cell division in the leaf growth zone through
154 promotion of JA accumulation. To do this, we used exogenous hormone treatments, hormone
155 biosynthesis and signaling mutants, kinematic analysis of leaf growth, and expression analysis.
156 Altogether, our data identified a previously unrecognized connection between cytokinin and the
157 defense hormone JA in regulating maize leaf growth.

158

159 RESULTS

160

161 ***Hsf1* mutants have a reduced growth phenotype.**

162 We have previously shown that *Hsf1/+* mutants have smaller leaves and that exogenous
163 CK treatment can phenocopy this effect (Muszynski et al., 2019) (Figure 1A, Supplemental
164 Figure S1). To further characterize this reduced growth phenotype, leaf size and growth rate
165 and duration of seedling leaf #4 was determined for *Hsf1/+* and wild type sibling plants in three
166 different genetic backgrounds (Figure 1A and B, Supplemental Figure S1). In all three
167 backgrounds, *Hsf1/+* leaf #4 blade length was reduced 10-20% compared to their wild type
168 siblings (Figure 1A, Supplemental Figure S1A). The B73 background was used for the
169 remainder of the studies. Consistent with a reduced blade size, leaf elongation rate (LER) was
170 also reduced by 20-25% across the three backgrounds (Figure 1B, Supplemental Figure S1B
171 and C). Interestingly, leaf elongation duration (LED) was slightly increased for *Hsf1/+* leaf #4
172 which may account for the fact that reduction in leaf size is not as great as the reduction in LER
173 would predict. To determine the cellular basis underlying this growth rate reduction, kinematic
174 analysis was performed on *Hsf1/+* and wild type siblings in the B73 genetic background
175 (Nelissen et al., 2013). Kinematic analysis showed that *Hsf1/+* mutants had fewer dividing cells
176 in the division zone and thus had a smaller division zone in leaf #4 compared to wild type
177 (Figure 1C). These data suggested that CK hypersignaling in *Hsf1/+* mutants reduced cell
178 divisions in the leaf growth zone, which slowed growth rate, resulting in a smaller leaf.

179

180 ***Hsf1/+* accumulates jasmonic acid in growing maize leaves.**

181 Plant hormones are known to exert their function through crosstalk with other hormones
182 (Santner and Estelle, 2009; De Vleeschauwer et al., 2014; Huot et al., 2014). To determine if
183 CK hypersignaling in the *Hsf1* mutant was affecting other hormones that may impact growth,
184 differences in phytohormone content were determined by high performance liquid
185 chromatography of WT and *Hsf1* whole seedlings. *Hsf1/+* accumulated 4-16-fold more of JA-Ile
186 and JA respectively compared to wild type (Figure 1D). A few other hormones showed modest
187 differential accumulation but not in a pattern consistent with the *Hsf1* reduced growth
188 phenotype. To obtain a better spatial resolution of the elevated JA content in *Hsf1*, mature leaf
189 blade #9 was sampled, divided into thirds along the proximal-distal axis, and JA content
190 determined. Consistent with the whole seedling data, JA content was elevated 2-3-fold across
191 the entire *Hsf1/+* leaf (Figure 1E). CK had not previously been shown to affect JA content but JA
192 was known to inhibit cell division in eudicots, and thus provided a possible mechanism by which

193 the *Hsf1* mutation conditioned reduced growth (Yamane et al., 1980; Zhang and Turner, 2008;
194 Noir et al., 2013). This prompted us to assess the effects of JA on maize leaf growth.

195

196 **JA pathway genes are upregulated in the leaf growth zone of *Hsf1* mutants.**

197 Given that JA content was increased in *Hsf1* mutants, we assessed whether the
198 expression of some JA pathway genes were increased in the *Hsf1* leaf growth zone. The growth
199 zone of leaf #4 at steady-state growth was partitioned into 5 mm subsections providing a high-
200 resolution spatial sampling through the division zone, first transition zone and elongation zone
201 (Figure 2). Subsections were collected in triplicate and transcript levels for select JA pathway
202 genes were measured by quantitative real-time PCR. These genes were chosen to broadly
203 survey key steps in JA biosynthesis and because mutants are available for some (Gao et al.,
204 2008; Yan et al., 2014) (Figure 2). We found the JA biosynthetic genes *ts1*, *ZmAOC2* and
205 *ZmOPR7* were significantly upregulated in the division zone of *Hsf1/+* (Figure 2). This
206 suggested that increased JA accumulation was due to increased expression of at least one JA
207 biosynthetic gene(s) in the division zone of *Hsf1* mutant leaves. In addition, the JA-responsive
208 gene *ZmMYC2* had higher expression throughout the entire growth zone in *Hsf1/+*, suggesting
209 increased JA levels were being perceived by the JA signaling pathway (Figure 2). Overall, the
210 expression data supports the hypothesis that CK signaling promotes JA accumulation through
211 increased expression of JA biosynthetic genes. However, we cannot discern the influence JA
212 feedback might have on these results. Since JA accumulation is increased in the growth zone of
213 *Hsf1* leaves and it is known that JA positively regulates its own biosynthesis (Pauwels et al.,
214 2009; Ahmad et al., 2016), we are not able to determine the specific influence CK has on JA
215 pathway gene expression in a “high” JA genotype.

216

217 **Exogenous jasmonic acid treatments reduce leaf growth rate in maize.**

218 To test if increased expression of JA biosynthetic genes could be responsible for
219 reduced leaf growth in the *Hsf1* mutant, B73 inbred maize seeds were transiently treated with 1
220 mM JA and effects on seedling leaf growth were assessed (see Materials & Methods for
221 details). Exogenous JA treatment of germinating maize seeds resulted in a 25-30% reduction in
222 sheath and blade length for seedling leaves #1 to #4 (Figure 3A, Supplemental Figure S2 and
223 Supplemental Table S1). JA treatment also promoted reductions in blade width which varied
224 between 9-20% depending on leaf number (Figure 3A and Supplemental Table S1). Similar to
225 effects of JA in other plant systems, these data indicated that JA treatment can reduce leaf size
226 in maize seedlings.

227 The JA mediated decrease in leaf size could have resulted from a reduction in growth
228 rate or the duration of growth or both. To distinguish the cause of leaf size reduction, the LER
229 and LED were determined for leaf #4 from B73 seedlings treated with JA, as described above.
230 While both control and JA treated plants maintained steady state growth for five days, JA-
231 treated seedlings had a pronounced reduction in LER compared to control throughout the period
232 of steady-state growth (Figure 3B). No obvious change in LED was observed. To determine the
233 minimum time of JA treatment required to elicit the observed growth reduction, germinating B73
234 seeds were treated with 1 mM JA for 1, 6, 12, 24 and 48 hours (see Methods for details).
235 Consistent decrease in blade length and width were observed only after 48 hours of JA
236 exposure for leaves #1 to #3 (Supplemental Figure S3 and Supplemental Table S2). Thus,
237 exogenous JA treatment for at least 48 hours could decrease maize leaf size by reducing
238 growth rate. These treatments supported a possible role of JA in reducing *Hsf1* growth rate.

239

240 ***Hsf1* is less responsive to exogenous jasmonic acid treatment.**

241 Because *Hsf1* mutant leaves have more JA and are smaller than wild type, we
242 hypothesized that leaf size of *Hsf1* mutants would be less responsive to exogenous JA
243 treatment than wild type siblings or the B73 inbred. To test this, we treated germinating seeds
244 that were segregating 50% *Hsf1*/+ and 50% wild type with 1 mM JA using the standard
245 germinating seed hormone assay. The excessive pubescence *Hsf1* phenotype (increased
246 macrohair density on the abaxial sheath) was not affected by exogenous JA treatments and was
247 100% concordant with previous molecular genotyping (data not shown). Thus it was a reliable
248 and reproducible method to score seedlings as either *Hsf1*/+ or wild type. As expected from
249 previous analysis, leaf size in untreated *Hsf1*/+ was reduced approximately 20% compared to
250 untreated wild type siblings (Figure 4A, Supplemental Table S3). JA treatment reduced leaf size
251 in both wild type and *Hsf1*/+ genotypes compared to their respective controls (Figure 4A).
252 However, the response to JA in *Hsf1*/+ plants was not as great as in the JA treated wild type
253 plants, as leaf size reduction was dependent on the leaf tissue and parameter measured. JA
254 treatment reduced wild type sheath length, blade length, and blade width about 15-25%, similar
255 to reductions seen in JA treated B73 seed, although blade #4 width was not affected (Figure 4A
256 and Supplemental Table S3). However, only blade length was consistently reduced (17-25%) in
257 JA-treated *Hsf1*/+ plants, with no reduction in sheath length and inconsistent reduction in blade
258 width (Figure 4A and Supplemental Table S3). These results suggest that in the *Hsf1*/+ mutant,
259 blade length but not the other leaf growth parameters are responsive to the JA treatment.

260 Since JA treatment further reduced *Hsf1/+* blade size, we asked if the JA treatment was
261 affecting growth rate or duration of growth. To do this, LER and LED were determined for leaf
262 #4 of seedlings from 1 mM JA treated 1:1 segregating *Hsf1* and wild type seeds (as above). As
263 seen previously, compared to untreated wild type sibs, untreated *Hsf1/+* had a reduced LER
264 and extended LED (Figure 4C). Also similar to our results with JA-treated B73, JA-treated wild
265 type LED was not affected but LER was reduced which was especially evident in the first 2.5
266 days of growth (Figure 4D). In contrast, *Hsf1/+* LER, especially during the first 2.5 days of
267 steady-state growth, was not affected by JA treatment. Instead, LED was reduced by JA
268 treatment in *Hsf1/+* plants where steady-state growth began to slow starting at 3 days, instead
269 of day 5, and continued to slow until leaf growth stopped by day 8 (Figure 4E). Comparing JA-
270 treated wild type and JA-treated *Hsf1/+* growth, showed a reduced LER but extended LED for
271 *Hsf1/+* plants, as was seen for these genotypes without JA treatment (Figure 4F). Thus,
272 although *Hsf1/+* blade length can be reduced further by JA treatment, it is likely caused by a
273 shortened LED, since LER was not impacted. This can be seen when comparing the actual leaf
274 length (sheath length + blade length) of growing leaf #4 from both genotypes with and without
275 JA treatment (Figures 4C to 4F). Leaf length was reduced at each time point during leaf growth
276 for wild type vs. *Hsf1/+*, for wild type vs. JA-treated wild type, and for JA-treated wild type vs.
277 JA-treated *Hsf1/+* (Figures 4C, 4D and 4F). In contrast, *Hsf1/+* vs. JA-treated *Hsf1/+* showed
278 leaf length was not different until after 7 days of leaf growth, nearly the time growth stopped
279 (Figure 3E). This suggests that in *Hsf1* mutants, where steady-state leaf growth is reduced,
280 possibly by increased JA content, additional JA can only further reduce leaf size by truncating
281 the duration of growth.

282

283 **Growth is enhanced in jasmonic acid-deficient mutants**

284 Our data are consistent with previous work showing JA can reduce growth. This implies
285 that reduced endogenous JA accumulation may enhance growth leading to larger leaves. To
286 understand how endogenous concentrations of JA might affect leaf growth and size, we
287 measured leaf size and growth in a number of maize JA deficient mutants (Yan et al., 2012;
288 Lunde et al., 2019). Duplicate genes encode 12-OXO-PHYTODIENOIC ACID REDUCTASE
289 (OPR), a key enzyme in the JA biosynthetic pathway responsible for converting OPDA into (+)-
290 7-iso-JA, which is later modified into bioactive JA (Yan et al., 2012). Plants homozygous for
291 recessive null mutations in both the *opr7* and *opr8* genes are JA deficient, display a feminized
292 tassel or “tasselseed” phenotype, and have longer seedling leaves #1 and #2 (Yan et al. 2012).
293 A single functional *opr* allele at either locus, renders that genotype wild type for JA content and

294 plant phenotype. Using a population that was homozygous null for *opr7* and segregating for a
295 wild type and null *opr8* alleles, we assessed leaf size and leaf growth in JA sufficient and JA
296 deficient genotypes (Figure 5A and 5B). As was shown previously, leaf #1 and #2 sheath and
297 blade lengths of the JA deficient genotype was increased 20%-48%, and leaf #3 and #4 blade
298 length was increased 13%-24% (Figure 5A and B and Supplemental Table S4). Interestingly,
299 sheath length was increased for leaf #3 but decreased in leaf #4 in the *opr7/opr7, opr8/opr8*
300 mutant (Supplemental Table S4). We also noted that blade width increased in leaf #3 and #4
301 9%-18% in the JA deficient genotype. Overall, in *opr7 opr8* double mutants, increases in sheath
302 and blade length diminished from leaf #1 to #4 but blade width changed from smaller to larger
303 than wild type. Assessment of growth rate in the double *opr7 opr8* mutant revealed an increase
304 in LER and LED compared to the JA-sufficient genotypes (Figure 5B). This suggested the lack
305 of JA increased both the rate and the duration of leaf growth.

306 To extend the results above, we also measured leaf size and growth in the semi-
307 dominant, gain-of-function *Tasselseed5* (*Ts5*) mutation (Lunde et al., 2019). The *Ts5* locus
308 encodes a cytochrome P450 enzyme, *ZmCYP94B1*, that oxidizes the bioactive JA-Ile to 12OH-
309 JA-Ile which is less bioactive and *Ts5* mutants express more *ZmCYP94B1* than wild type
310 (Lunde et al., 2019). Thus, *Ts5/+* plants have a lower JA content than wild type sibs and display
311 the tasselseed phenotype expected for JA deficient mutants. *Ts5/+* was crossed to *Hsf1/+* and
312 the 1:1:1:1 segregating population was analyzed for LER and LED. LER and LED was
313 measured and plants were genotyped for *Ts5/+*. First we analyzed *Ts5/+* growth compared to
314 wild type. *Ts5/+* plants exhibited increased LER compared to wild type and possibly an increase
315 in growth duration (Figure 5C). Consistent with the results from the *opr7 opr8* population, these
316 JA deficient mutants showed increased growth rate, supporting the role of reduced JA
317 promoting leaf growth.

318

319 **JA-deficient mutants suppress the reduced leaf growth phenotype in *Hsf1* mutants.**

320 Using the population described in Figure 5C, we next compared the LER and LED of
321 single and double mutants. *Hsf1/+* mutants had reduced LER and an extended LED compared
322 to wild type as seen from previous characterization of *Hsf1/+* growth (Figure 1B, Supplemental
323 Figure 1B and C). *Ts5/+* as stated in Figure 5C, had increased LER compared to WT.
324 Interestingly, the average LER for the double mutant *Hsf1/+ Ts5/+* closely matched wild type
325 except for at the 48 hr time point where WT LER slightly exceeded the *Hsf1/+ Ts5/+* LER.
326 (Figure 6A). Analysis of the final leaf lengths of the entire population showed crossing *Hsf1/+* to

327 *Ts5/+* reduced final leaf length to wild type lengths (Figure 6B). *Ts5/+* exhibited a wild type
328 LER and LED growth pattern (Figure 6A).

329

330 **Exogenous CK treatment induces expression of JA pathway genes in the leaf growth**
331 **zone.**

332 Since the expression of several JA pathway genes was higher in the leaf GZ of the
333 *Hsf1* CK hypersignaling mutant, we asked if exogenous CK application of maize inbred
334 seedlings could also induce JA pathway expression in the leaf GZ. To do this, 10-day old B73
335 seedlings were cut at the root:shoot junction, and shoots were incubated for 1, 2 and 4 hours
336 with 10 μ M 6-BAP (details in Methods). After incubation, the basal 2 cm of leaf #4,
337 encompassing the DZ and part of the EZ, was collected, and JA pathway expression was
338 quantified using qRT-PCR. We first determined that the exogenous CK application was
339 perceived by assessing expression of three CK early response genes: the type A response
340 regulators *ZmRR3* and *ZmRR6*, and *cytokinin oxidase2 (ckx2)*. Type A response regulators are
341 negative regulators of CK signaling that are rapidly expressed without *de novo* protein synthesis
342 upon CK treatment (To et al., 2004; Ferreira and Kieber, 2005). As expected, *ZmRR6*
343 transcripts were upregulated in the GZ by 1 hour, and all three CK reporters showed robust
344 expression by 4 hours (Figure 7A). Thus, the GZ of leaf #4 was perceiving and responding to
345 the CK application by 4 hours. We next assessed JA pathway expression in these same tissues.
346 Of the genes surveyed, we found an increase in expression of both JA biosynthesis and
347 catabolism genes. Specifically, *ts1*, *aos1a*, *aos2a*, *aoc2*, *opr7*, and *Ts5* all showed a 1.5 to 3
348 fold increase in expression after 4 hrs of CK treatment. This showed that CK could induce JA
349 pathway gene expression in the maize leaf GZ after 4 hours.

350 We next asked if the CK-induced increase in JA gene expression required new protein
351 synthesis downstream of CK signaling. We considered two possibilities: 1) CK treatment and
352 subsequent signaling resulted in the downstream phosphorylation and activation of a
353 transcription factor, such as a type-B response regulator or 2) CK treatment and signaling
354 resulted in the transcription and translation of a new transcription factor that activated
355 expression of the upregulated JA genes. To do this, CK application on cut B73 seedling shoots
356 was repeated with and without cyclohexamide (CHX), a translational blocker. We hypothesized
357 that if CK-induced expression of JA genes was dependent on *de novo* protein synthesis,
358 combined treatment with CK and CHX would result in no increased expression of JA-pathway
359 genes. However, if any JA genes were directly regulated by CK signaling components, like
360 expression of *ZmRR3* and *ZmRR6*, JA gene expression would still be increased in the

361 combined CK and CHX treated samples. We first tested that the combined CK and CHX
362 treatment would work as expected by assessing expression of the three CK reporters. As
363 expected, since type-A response regulator expression does not require *de novo* protein
364 synthesis, *ZmRR3* and *ZmRR6* expression increased in the combined CK and CHX treatment,
365 although the increase was less than with CK alone (Figure 6B). In contrast, the CK-induced
366 increased expression of JA pathway genes was abolished with CHX treatment (Figure 6B). This
367 suggests that CK induces transcription and translation of a new protein that regulates JA
368 biosynthesis gene expression in the leaf GZ. Our CK-induction system will be very useful in
369 identifying the CK-induced regulators of these JA pathway genes.

370

371

372 **DISCUSSION**

373

374 Many dicot examples show that CK signaling promotes the accumulation of plant
375 biomass (Werner et al., 2001; Riefler et al., 2006; Bartrina et al., 2017). *Hsf1*, a monocot, does
376 not follow this pattern and instead shows reduced shoot growth (Muszynski et al., 2019) (Figure
377 1A and B). In contrast to the constitutive CK receptor mutant in *Arabidopsis*, which has larger
378 leaves with more cells, *Hsf1* has smaller leaves due to a smaller division zone and reduced
379 number of dividing cells (Bartrina et al., 2017) (Figure 1C). Due to the lack of CK signaling
380 mutants in monocots, it is difficult to tell if differential CK-mediated growth responses in
381 monocots and dicots mark true differences in CK signaling or are due to absolute differences in
382 endogenous CK concentrations and perception. However, rice *OsIPT3* transformants
383 overexpressing the rate limiting CK biosynthesis enzyme IPT3, resulted in stunted plants and is
384 another example of excess CK reducing plant growth (Sakamoto et al., 2006).

385 To understand the connection between CK and leaf growth in *Hsf1*, we focused on
386 characterizing the role of JA in regulating maize leaf growth because of its accumulation in *Hsf1*
387 (Figure 1D and E) and the differential expression of JA biosynthesis genes in the division zone
388 (Figure 2). Previous research has established that monocot and dicot growth is reduced through
389 JA-mediated inhibition of cell proliferation (Yamane et al., 1980; Zhang and Turner, 2008; Noir
390 et al., 2013; Yan et al., 2014). As expected, exogenous application of JA to maize reduced LER
391 which ultimately reduced leaf size (Figure 3A and B). Interestingly, analysis of mutants deficient
392 in JA (*opr7 opr8* and *Ts5*) show increased final leaf size due to increased LER and LED (Yan et
393 al., 2014) (Figure 5). These data show that JA impacts growth primarily by decreasing LER, and
394 support the role of JA mediated growth reduction in *Hsf1* leaves.

395 Our data suggests that CK hypersignaling induces growth reduction in maize by
396 crosstalk with the growth repressor, JA (Figure 7). Crosstalk between CK and JA is not well
397 characterized and previous data linking the two has been indirect (Ueda and Kato, 1982;
398 Dermastia et al., 1994; O'Brien and Benková, 2013). The majority of these studies relied on
399 exogenous treatments of CK and JA with mixed results that indicated a complex relationship
400 between the two hormones (Ueda and Kato, 1982; Dermastia et al., 1994; O'Brien and
401 Benková, 2013). However, the earliest of these studies observed that JA treatment antagonized
402 CK mediated callus growth (Ueda and Kato, 1982). Our double mutant analysis of *Hsf1/+ Ts5/+*
403 reflect an antagonistic relationship between JA and CK, as the double mutant had wild type LER
404 and final leaf length (Figure 6A and B). In addition, we found that CK treatment of B73 seedlings
405 promotes the transcription and translation of an unidentified protein that promotes the
406 expression of JA biosynthesis genes (Figure 7A and B). Further studies are needed to identify
407 the CK-inducible regulators of the described JA genes.

408 JA treatments of *Hsf1* suggest that CK crosstalk with other hormones in addition to JA
409 may also play a role in controlling *Hsf1* growth. While crossing the *Ts5/+* with *Hsf1/+* rescued
410 the reduced growth phenotype of *Hsf1/+*, the *Hsf1/+* growth pattern could not be phenocopied
411 with exogenous JA treatment (Figure 4F). These data show that JA treatment reduces wild type
412 leaf size to be equivalent with *Hsf1* (Figure 4A and B) and suggests that JA also reduces leaf
413 size by shortening leaf elongation duration (Figure 4E). Differences between the *Hsf1/+ Ts5/+*
414 cross and the exogenous JA treatment of *Hsf1/+* may stem from strength of JA perception or
415 reveal the presence of another hormone that crosstalks with CK and JA. Specifically, the
416 extended LED growth pattern is similar to that of a GA signaling mutant, and provides another
417 avenue of hormone crosstalk to investigate in the *Hsf1/+* mutant (Nelissen et al., 2012). Taken
418 together, it is likely that JA is responsible for reducing LER, and another hormone controls LED
419 in *Hsf1*.

420

421 **Conclusion**

422

423 In conclusion, these data suggest that CK hypersignaling upregulates JA biosynthesis
424 genes, leading to growth reduction in the maize *Hsf1* leaf by suppressing cell proliferation. We
425 provide evidence for an unidentified CK-inducible protein regulator that targets JA biosynthesis
426 genes. Additionally, growth analysis of JA-treated plants and JA-deficient mutants show that JA
427 impacts leaf growth by reducing LER, and removal of JA promotes leaf growth by increasing
428 LER. Collectively, these data highlight a new connection between CK and JA. Determining how

429 CK connects to JA has the potential to provide new insights into the mechanisms plants use to
430 balance growth and defense.
431

432 MATERIALS AND METHODS

433

434 Plant Material, Genetics, Phenotypic Measurements, and Analysis

435 Inbred B73 was used as the standard maize line for all seed and seedling treatments. The CK
436 hypersignaling mutant *Hsf1-1603* was previously described (Muszynski et al., 2019). The JA-
437 deficient *opr7-5 opr8-2* (we will refer to it as *opr7 opr8*) and *Tasselseed 5 (Ts5)* was previously
438 described in Yan *et al.* 2012 and Lunde *et al.* 2005 respectively (Yan et al., 2012; Lunde et al.,
439 2019). *Hsf1/+* plants were identified by the presence of macrohairs at the V1 stage and prongs
440 in leaf margins past V6 (Muszynski et al., 2019). JA-deficient mutants were grown in flats and
441 genotyped by PCR using the primers described in Supplemental Table S5. Plants were crossed
442 for several generations to produce the following genotypes to analyze: [+/, *opr7, opr8/+*] WT,
443 [*Hsf1/+*, *opr7, opr8/+*] CK-hypersignaling only, [+/, *opr7, opr8*] JA-deficient only, and [*Hsf1/+*,
444 *opr7, opr8*] CK hypersignaling JA-deficient plants. In parallel, genotypes: [+/, *ts1/+*] WT,
445 [*Hsf1/+*, *ts1/+*], CK hypersignaling only, [+/, *ts1*] JA-deficient, and [*Hsf1/+*, *ts1*] CK
446 hypersignaling JA-deficient plants were developed. All genotypic classes were grown until leaf 4
447 matured.

448

449 Standard Germinating Seed Hormone Treatment

450 A stock and control solution of hormone was made as described by the manufacturer and stored
451 at -80°C. Surface sterilized seeds imbibed overnight were placed embryo-face down, about 20
452 seeds/petri dish, onto a sterile paper towel and soaked with 2.5 mL of hormone at a working
453 concentration (varied by hormone) in a 15 mm petri dish. Typically, three biological replicates
454 were done per treatment, using 20 seeds/petri dish X 3 = 60 total seeds/treatment. The edges
455 of the petri dishes were sealed with parafilm to prevent evaporation and the entire petri dish was
456 wrapped in foil and placed in a lab drawer for six days. After six days of treatment, germinated
457 seedlings were removed from the petri dish, rinsed with sterile tap water, and transplanted to 1
458 gallon pots (Sunshine Mix #4 media, supplemented with 2 teaspoons osmocote, 2 teaspoons
459 ironite) and placed in the Pope greenhouse.

460

461 Cytokinin

462 6-Benzylaminopurine (6-BAP) powder from Sigma Aldrich was first dissolved in 10 drops of 1 N
463 NaOH, and brought to a concentration of 10 mM with sterile distilled water. A parallel water
464 control stock was also made with 10 drops of 1N NaOH. These stocks were further diluted to
465 achieve the desired hormone treatment concentrations.

466

467 **Jasmonic Acid**

468 100 mg of JA (Sigma-Aldrich) was dissolved in 3 mL of 200-proof ethanol and 44.5 mL of sterile
469 ddH₂O to make a stock concentration of 10 mM JA. A control solution was made by adding 3
470 mL of 200 proof ethanol to 44.5 mL of ddH₂O and stored at -80°C. Both the JA and control
471 solutions were diluted with sterile ddH₂O until the desired working solution concentration was
472 reached. Stock solutions were stored at -80°C in 15 mL tubes. The working solution was made
473 the day treatments started by diluting the 10 mM stock with sterile ddH₂O to a final volume of
474 2.5 mL/petri dish.

475

476 **Final Leaf Size Measurements**

477 Treated seedlings were grown until the fifth leaf was completely collared (the auricle and ligule
478 that defines the junction between the leaf sheath and blade was visible), ensuring that leaves #1
479 to #4 had completed growth. Sheath length, blade length, and blade width were measured for
480 leaves #1 (most basal, first formed) to leaf #4. Leaves were measured by harvesting each leaf
481 at its insertion into the stem. For sheath length— length was measured from the base of the
482 sheath to the point at which the sheath transitions to the auricle at the midline of the leaf. For
483 blade length— length was measured along the midrib from the auricle to the distal blade tip. For
484 blade width— width was measured at the midpoint of blade length across the blade from margin
485 to margin.

486

487 **Growth Rate Measurement**

488 Leaf elongation rates (LER) were taken when leaf #4 emerged from the whorl and was at
489 steady-state growth, when LER is constant (Sun et al., 2017). Briefly, the length of leaf #4 was
490 measured as the distance from the insertion point of leaf #1 at the base of the plant to the tip of
491 leaf #4 every 12 or 24 hours until leaf #4 stopped growth (leaf length did not change for 2-3
492 consecutive time points). LER was calculated by dividing the difference in leaf length (cm) by
493 the time elapsed (24 hrs). Leaf elongation duration (LED), the measure of time from when the
494 leaf is 10 cm to final length, was determined from plotting LER by time elapsed. Leaf elongation
495 duration (LED) was determined when steady state growth stopped as observed when plotting
496 LER by days post leaf 4 emergence from the whorl. Finally, plants were dissected and leaf
497 blade length, leaf blade width (measure at ½ the blade length mark), and leaf sheath length
498 were measured on leaves #1 – 4.

499

500

501 **Seedling treatments and JA-pathway gene expression analysis**

502 Seedling treatments were performed as described in (Giulini et al., 2004) on B73 seedlings
503 when leaf 4 was emerging from the whorl. Briefly, individual seedlings were cut at the shoot-root
504 junction and submerged in 500 μ L of 10 μ M 6-BAP or equivalent control for 4 hrs. The basal 2
505 cm of the leaf, where division and expansion occurs, was dissected and put in 500 μ L of IBI
506 Isolate (IBI Scientific, CAT: IB47601) for RNA extraction following the manufacturer's
507 recommendations. RNA was quantified by using ND-1000 Spectrophotometer (Nanodrop,
508 Wilmington, DE). A total of 2 μ g of RNA was used to synthesize cDNA with SuperScript IV VIL0
509 Master Mix with ezDNase Enzyme kit (Thermo Fisher Scientific, CAT: 11766050) following the
510 manufacturer's recommendations. Finally, 1:10 dilution of cDNA was used for RT- and
511 quantitative RT-PCR.

512

513 Samples were initially screened for CK perception by RT-PCR amplifying *ZmRR3* (*abph1*;
514 Zm00001d002982), a type-A response regulator that is only expressed when CK is present
515 (Giulini et al., 2004), using the EconoTaq® PLUS GREEN 2X Master Mix (Lucigen; Middleton,
516 WI) and following the manufacturer's recommendations. The RT-PCR was performed using
517 S1000™ Thermal Cyclers (Bio-Rad; Hercules, CA) using the following cycling program: step 1 =
518 98 °C for 2 min, step 2 = 98 °C for 30 sec, step 3 = 60 °C for 30 sec, step 4 = 72 °C for 30 sec,
519 step 5 = repeat steps 2 – 4 29 times, step 6 = 72 °C for 5 min, and step 7 = 10 °C. PCR
520 products were run in 2% agarose gel electrophoresis using a 100 bp DNA ladder (GenScript;
521 CAT: M1020).

522

523 Once perception was confirmed, genes that encode for the biosynthetic enzymes along the JA-
524 pathway were evaluated by quantitative RT-PCR using the iQ SYBR Green Supermix (Bio-Rad;
525 CAT: 1708882) reagents, following manufacturer recommendations, and Bio-Rad CFX96
526 Touch™ thermocycler (Bio-Rad; Hercules, CA) with primers listed in Supplemental Table 5. C_q
527 values were used to calculate Fold Change differences between the control and the treatments
528 following (Livak and Schmittgen, 2001) and calculating significant differences using Student's t-
529 test.

530

531

532 **Hormone Analysis**

533

534 **Plant metabolite assays**

535 Plant hormones (cytokinins, jasmonate, salicylic acid, auxin, *cis*-zeatin, *trans*-zeatin) were
536 measured by HPLC-mass spectrometry (HPLC-MS) as described previously (Schäfer et al.,
537 2016).

538

539

540

541 **ACKNOWLEDGEMENTS**

542

543 We would like to thank all past and present members of the Muszynski Lab for their help in data
544 collection including Dylan Oates, Miranda Yip, Bridnie Hill, Jessica Szyska and Sirut Buasai.

545 ANU was awarded a Syngenta Agricultural Scholarship.

546

547 Hormone profiling done by GJ was funded by US National Science Foundation award 1339237
548 and a Friedrich Wilhelm Bessel Research Award from the Humboldt Foundation.

549

550

551

552

553 **LITERATURE CITED**

554

555 **Acosta IF, Laparra H, Romero SP, Schmelz E, Hamberg M, Mottinger JP, Moreno MA,**
556 **Dellaporta SL** (2009) tasselseed1 is a lipoxygenase affecting jasmonic acid signaling in
557 sex determination of maize. *Science* **323**: 262–265

558 **Ahmad P, Rasool S, Gul A, Sheikh SA, Akram NA, Ashraf M, Kazi AM, Gucel S** (2016)
559 Jasmonates: Multifunctional Roles in Stress Tolerance. *Front Plant Sci* **7**: 813

560 **Bartrina I, Jensen H, Novák O, Strnad M, Werner T, Schmölling T** (2017) Gain-of-Function
561 Mutants of the Cytokinin Receptors AHK2 and AHK3 Regulate Plant Organ Size, Flowering
562 Time and Plant Longevity. *Plant Physiol* **173**: 1783–1797

563 **Bertrand-Garcia R, Freeling M** (1991) HAIRY-SHEATH FRAYED #1-O: A SYSTEMIC,
564 HETEROCHRONIC MUTANT OF MAIZE THAT SPECIFIES SLOW DEVELOPMENTAL
565 STAGE TRANSITIONS. *Am J Bot* **78**: 747–765

566 **Conklin PA, Strable J, Li S, Scanlon MJ** (2019) On the mechanisms of development in
567 monocot and eudicot leaves. *New Phytol* **221**: 706–724

568 **Dermastia M, Ravnikar M, Vilhar B, Kovac M** (1994) Increased level of cytokinin ribosides in
569 jasmonic acid-treated potato (*Solanum tuberosum*) stem node cultures. *Physiol Plant* **92**:
570 241–246

571 **De Vleeschauwer D, Xu J, Höfte M** (2014) Making sense of hormone-mediated defense
572 networking: from rice to Arabidopsis. *Front Plant Sci* **5**: 611

573 **Ferreira FJ, Kieber JJ** (2005) Cytokinin signaling. *Curr Opin Plant Biol* **8**: 518–525

574 **Frébort I, Kowalska M, Hluska T, Frébortová J, Galuszka P** (2011) Evolution of cytokinin
575 biosynthesis and degradation. *J Exp Bot* **62**: 2431–2452

576 **Gao X, Starr J, Göbel C, Engelberth J, Feussner I, Tumlinson J, Kolomiets M** (2008) Maize
577 9-lipoxygenase ZmLOX3 controls development, root-specific expression of defense genes,
578 and resistance to root-knot nematodes. *Mol Plant Microbe Interact* **21**: 98–109

579 **Giulini A, Wang J, Jackson D** (2004) Control of phyllotaxy by the cytokinin-inducible response
580 regulator homologue ABPHYL1. *Nature* **430**: 1031–1034

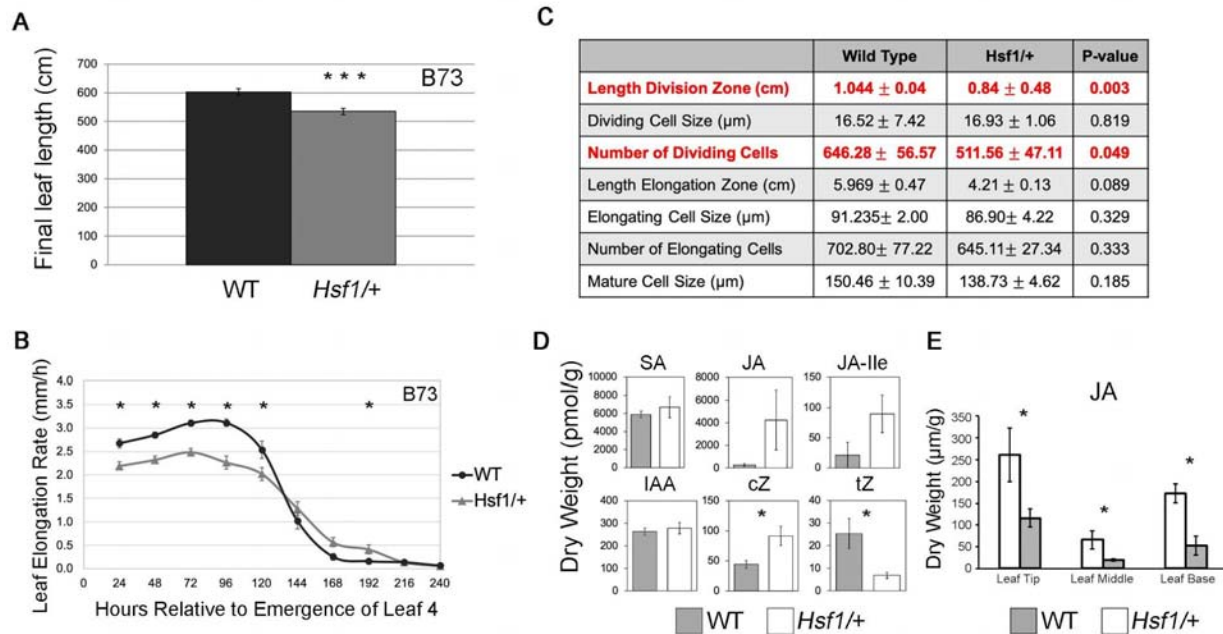
- 581 **Gupta MD, Nath U** (2016) On the evolution of developmental mechanisms: Divergent polarities
582 in leaf growth as a case study. *Plant Signal Behav* **11**: e1126030
- 583 **Hou X, Ding L, Yu H** (2013) Crosstalk between GA and JA signaling mediates plant growth and
584 defense. *Plant Cell Rep* **32**: 1067–1074
- 585 **Huot B, Yao J, Montgomery BL, He SY** (2014) Growth-defense tradeoffs in plants: a balancing
586 act to optimize fitness. *Mol Plant* **7**: 1267–1287
- 587 **Kiesselbach TA** (1999) The Structure and Reproduction of Corn, 50th Anniv. 30–37
- 588 **Livak KJ, Schmittgen TD** (2001) Analysis of Relative Gene Expression Data Using Real- Time
589 Quantitative PCR and the 2^{-ΔΔC_T} Method. *Methods* **25**: 402–408
- 590 **Lomin SN, Yonekura-Sakakibara K, Romanov GA, Sakakibara H** (2011) Ligand-binding
591 properties and subcellular localization of maize cytokinin receptors. *J Exp Bot* **62**: 5149–
592 5159
- 593 **Lunde C, Kimberlin A, Leiboff S, Koo AJ, Hake S** (2019) Tasselseed5 overexpresses a
594 wound-inducible enzyme, ZmCYP94B1, that affects jasmonate catabolism, sex
595 determination, and plant architecture in maize. *Commun Biol* **2**: 114
- 596 **Lyons R, Manners JM, Kazan K** (2013) Jasmonate biosynthesis and signaling in monocots: a
597 comparative overview. *Plant Cell Rep* **32**: 815–827
- 598 **Miller CO, Skoog F, Von Saltza MH, Strong FM** (1955) KINETIN, A CELL DIVISION FACTOR
599 FROM DEOXYRIBONUCLEIC ACID1. *J Am Chem Soc* **77**: 1392–1392
- 600 **Muszynski MG, Moss-Taylor L, Chudalayandi S, Cahill J, Del Valle-Echevarria AR, Alvarez**
601 **I, Petefish A, Makita N, Sakakibara H, Krivosheev DM, et al** (2019) The maize Hairy
602 Sheath Frayed1 (Hsf1) mutant alters leaf patterning through increased cytokinin signaling.
603 bioRxiv 743898
- 604 **Nelissen H, Gonzalez N, Inzé D** (2016) Leaf growth in dicots and monocots: so different yet so
605 alike. *Curr Opin Plant Biol* **33**: 72–76
- 606 **Nelissen H, Rymer B, Coppens F, Dhondt S, Fiorani F, Beemster GTS** (2013) Kinematic
607 Analysis of Cell Division in Leaves of Mono- and Dicotyledonous Species: A Basis for
608 Understanding Growth and Developing Refined Molecular Sampling Strategies. *In I De*

- 609 Smet, ed, *Plant Organogenesis: Methods and Protocols*. Humana Press, Totowa, NJ, pp
610 247–264
- 611 **Nelissen H, Rymen B, Jikumaru Y, Demuyne K, Van Lijsebettens M, Kamiya Y, Inzé D,**
612 **Beemster GTS** (2012) A local maximum in gibberellin levels regulates maize leaf growth by
613 spatial control of cell division. *Curr Biol* **22**: 1183–1187
- 614 **Noir S, Bömer M, Takahashi N, Ishida T, Tsui T-L, Balbi V, Shanahan H, Sugimoto K,**
615 **Devoto A** (2013) Jasmonate controls leaf growth by repressing cell proliferation and the
616 onset of endoreduplication while maintaining a potential stand-by mode. *Plant Physiol* **161**:
617 1930–1951
- 618 **O’Brien JA, Benková E** (2013) Cytokinin cross-talking during biotic and abiotic stress
619 responses. *Front Plant Sci* **4**: 451
- 620 **Pauwels L, Inzé D, Goossens A** (2009) Jasmonate-inducible gene: What does it mean?
621 *Trends Plant Sci* **14**: 87–91
- 622 **Pineda Rodo A, Brugière N, Vankova R, Malbeck J, Olson JM, Haines SC, Martin RC,**
623 **Habben JE, Mok DWS, Mok MC** (2008) Over-expression of a zeatin O-glucosylation gene
624 in maize leads to growth retardation and tasselseed formation. *J Exp Bot* **59**: 2673–2686
- 625 **Riefler M, Novak O, Strnad M, Sch Müller T** (2006) Arabidopsis cytokinin receptor mutants
626 reveal functions in shoot growth, leaf senescence, seed size, germination, root
627 development, and cytokinin metabolism. *Plant Cell* **18**: 40–54
- 628 **Sakamoto T, Sakakibara H, Kojima M, Yamamoto Y, Nagasaki H, Inukai Y, Sato Y,**
629 **Matsuoka M** (2006) Ectopic expression of KNOTTED1-like homeobox protein induces
630 expression of cytokinin biosynthesis genes in rice. *Plant Physiol* **142**: 54–62
- 631 **Santner A, Estelle M** (2009) Recent advances and emerging trends in plant hormone
632 signalling. *Nature* **459**: 1071–1078
- 633 **Schäfer M, Brütting C, Baldwin IT, Kallenbach M** (2016) High-throughput quantification of
634 more than 100 primary- and secondary-metabolites, and phytohormones by a single solid-
635 phase extraction based sample preparation with analysis by UHPLC-HESI-MS/MS. *Plant*
636 *Methods* **12**: 30

- 637 **Steklov MY, Lomin SN, Osolodkin DI, Romanov GA** (2013) Structural basis for cytokinin
638 receptor signaling: an evolutionary approach. *Plant Cell Rep* **32**: 781–793
- 639 **Sun X, Cahill J, Van Haute gem T, Feys K, Whipple C, Novák O, Delbare S, Versteele C,**
640 **Demuy nck K, De Block J, et al** (2017) Altered expression of maize PLASTOCHRON1
641 enhances biomass and seed yield by extending cell division duration. *Nat Commun* **8**:
642 14752
- 643 **To JPC, Haberer G, Ferreira FJ, Deruère J, Mason MG, Schaller GE, Alonso JM, Ecker JR,**
644 **Kieber JJ** (2004) Type-A Arabidopsis response regulators are partially redundant negative
645 regulators of cytokinin signaling. *Plant Cell* **16**: 658–671
- 646 **Ueda J, Kato J** (1982) Inhibition of cytokinin-induced plant growth by jasmonic acid and its
647 methyl ester. *Physiol Plant* **54**: 249–252
- 648 **Wang D, Pajeroska-Mukhtar K, Culler AH, Dong X** (2007) Salicylic acid inhibits pathogen
649 growth in plants through repression of the auxin signaling pathway. *Curr Biol* **17**: 1784–
650 1790
- 651 **Werner T, Motyka V, Strnad M, Schmülling T** (2001) Regulation of plant growth by cytokinin.
652 *Proc Natl Acad Sci U S A* **98**: 10487–10492
- 653 **Wolters H, Jürgens G** (2009) Survival of the flexible: hormonal growth control and adaptation
654 in plant development. *Nat Rev Genet* **10**: 305–317
- 655 **Yamane H, Sugawara J, Suzuki Y, Shimamura E, Takahashi N** (1980) Syntheses of jasmonic
656 acid related compounds and their structure-activity relationships on the growth of rice
657 seedlings. *Agric Biol Chem* **44**: 2857– 2864
- 658 **Yan Y, Christensen S, Isakeit T, Engelberth J, Meeley R, Hayward A, Emery RJN,**
659 **Kolomiets MV** (2012) Disruption of OPR7 and OPR8 reveals the versatile functions of
660 jasmonic acid in maize development and defense. *Plant Cell* **24**: 1420–1436
- 661 **Yan Y, Huang P-C, Borrego E, Kolomiets M** (2014) New perspectives into jasmonate roles in
662 maize. *Plant Signal Behav* **9**: e970442
- 663 **Zhang Y, Turner JG** (2008) Wound-induced endogenous jasmonates stunt plant growth by
664 inhibiting mitosis. *PLoS One* **3**: e3699

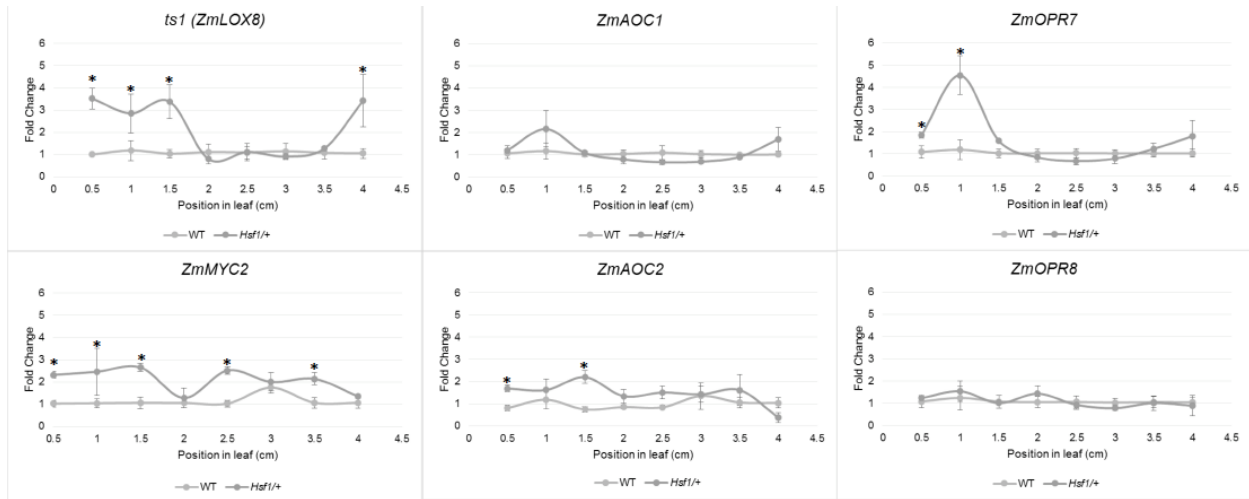
665

666



667
 668 **Figure 1.** *Hsf1* growth and phytohormone phenotypes. **(A)** Barplots of WT and *Hsf1/+* final leaf
 669 lengths. Error bars = SE. **(B)** Average leaf elongation rate (LER) of leaf #4 of *Hsf1/+* and WT-
 670 siblings in the B73 inbred background. Asterisks mark significant difference $P < 0.05$. Error bars
 671 = SE. **(C)** Kinematic analysis comparing growth zones of the *Hsf1/+* mutant and its WT-sibling.
 672 **(D)** Two-week old whole-seedling hormone profile of *Hsf1/+* and WT-siblings. SA, Salicylic Acid;
 673 JA, Jasmonic Acid; JA-Ile, Jasmonic Acid Isoleucine; IAA, Indole-3-Acetic Acid; cZ, *cis*-Zeatin;
 674 tZ, *trans*-Zeatin. **(E)** Jasmonic Acid (JA) concentration across leaf nine at steady-state growth.
 675 The leaf was divided into three sections (leaf base, leaf middle, and leaf tip). Leaf base includes
 676 the growth zone. White columns are *Hsf1/+* and gray columns are WT-sibling.
 677
 678

679



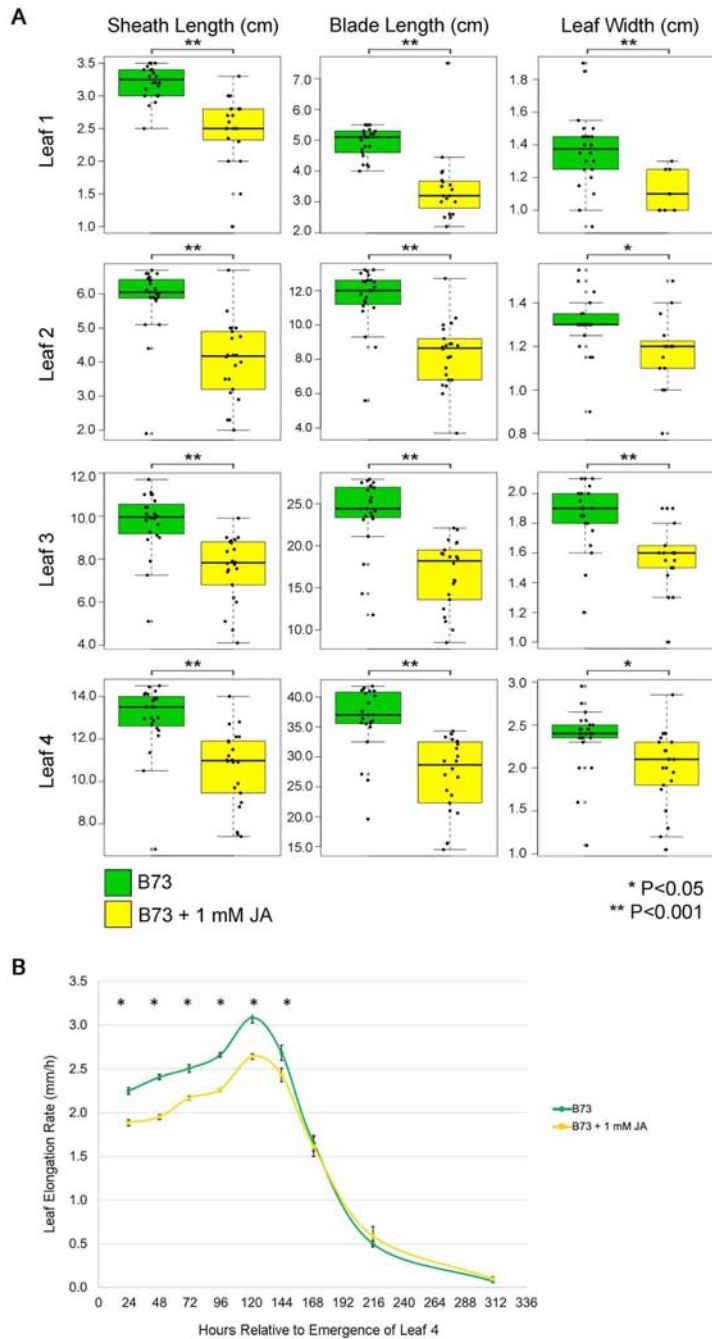
680

681 **Figure 2.** JA pathway genes are up-regulated in the growth zone of *Hsf1* leaves. RT-qPCR of
682 key JA biosynthesis and signaling genes across the division zone in *Hsf1/+* and wild type leaf
683 #4 at steady state growth.

684

685

686

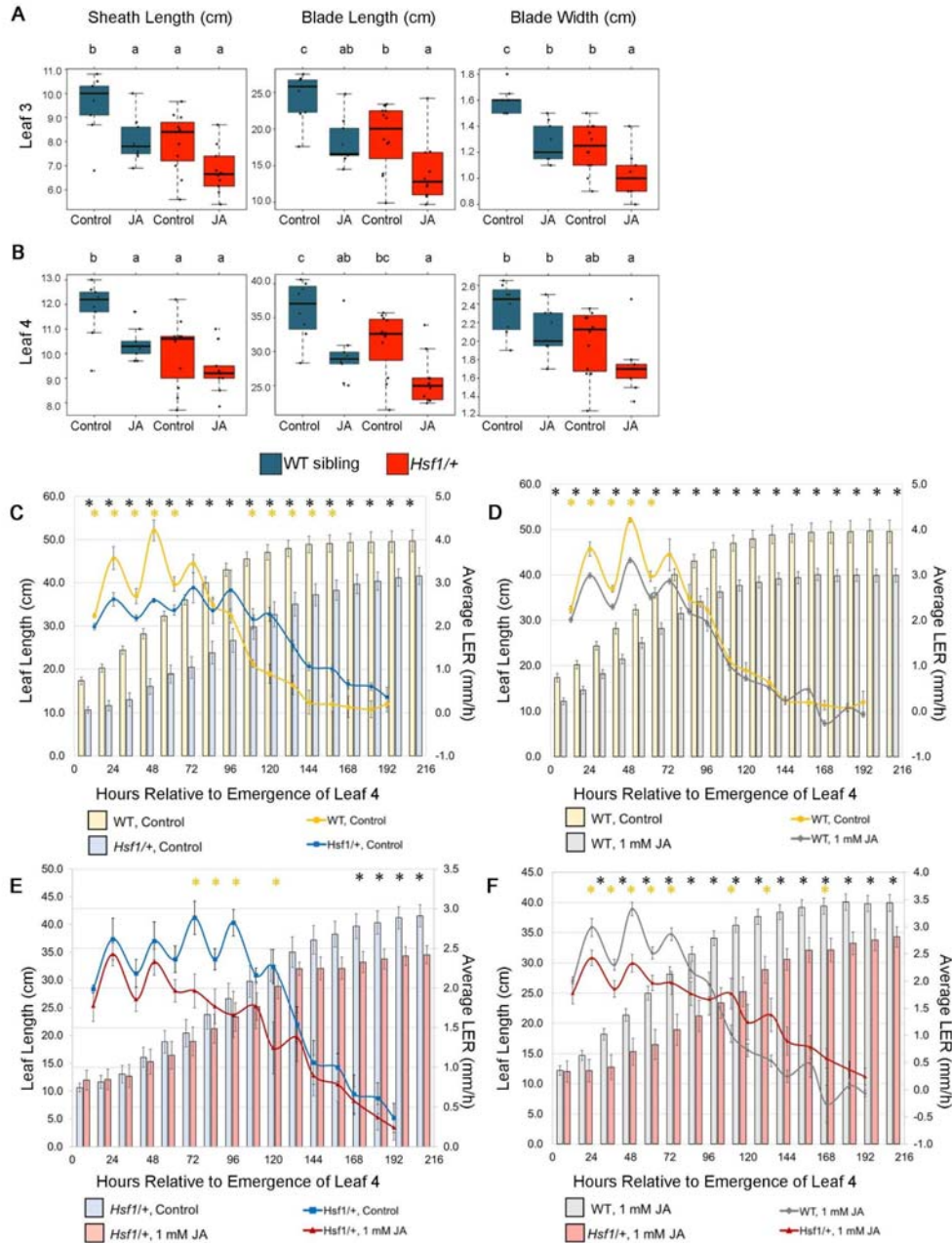


687

688 **Figure 3.** Effect of JA on B73 growth. **(A)** Boxplots of sheath length, blade length, and blade
689 width in control and 1 mM JA treatments of leaf #1-4. Horizontal bars represent the maximum,
690 third quantile, median, first quantile, and minimum values respectively. Each dot is a plant (B73,
691 n=23; B73 + JA, n=22). **(B)** Average leaf elongation rate (LER) of leaf #4 at steady-state growth

692 of seedlings in control compared to 1 mM JA treatment groups. Error bars = SE. Asterisks mark
693 significant differences of LER between treatments at each time point by Student's t-test p-value
694 ≤ 0.05 (B73, n=27; B73 + JA; n=22).

695



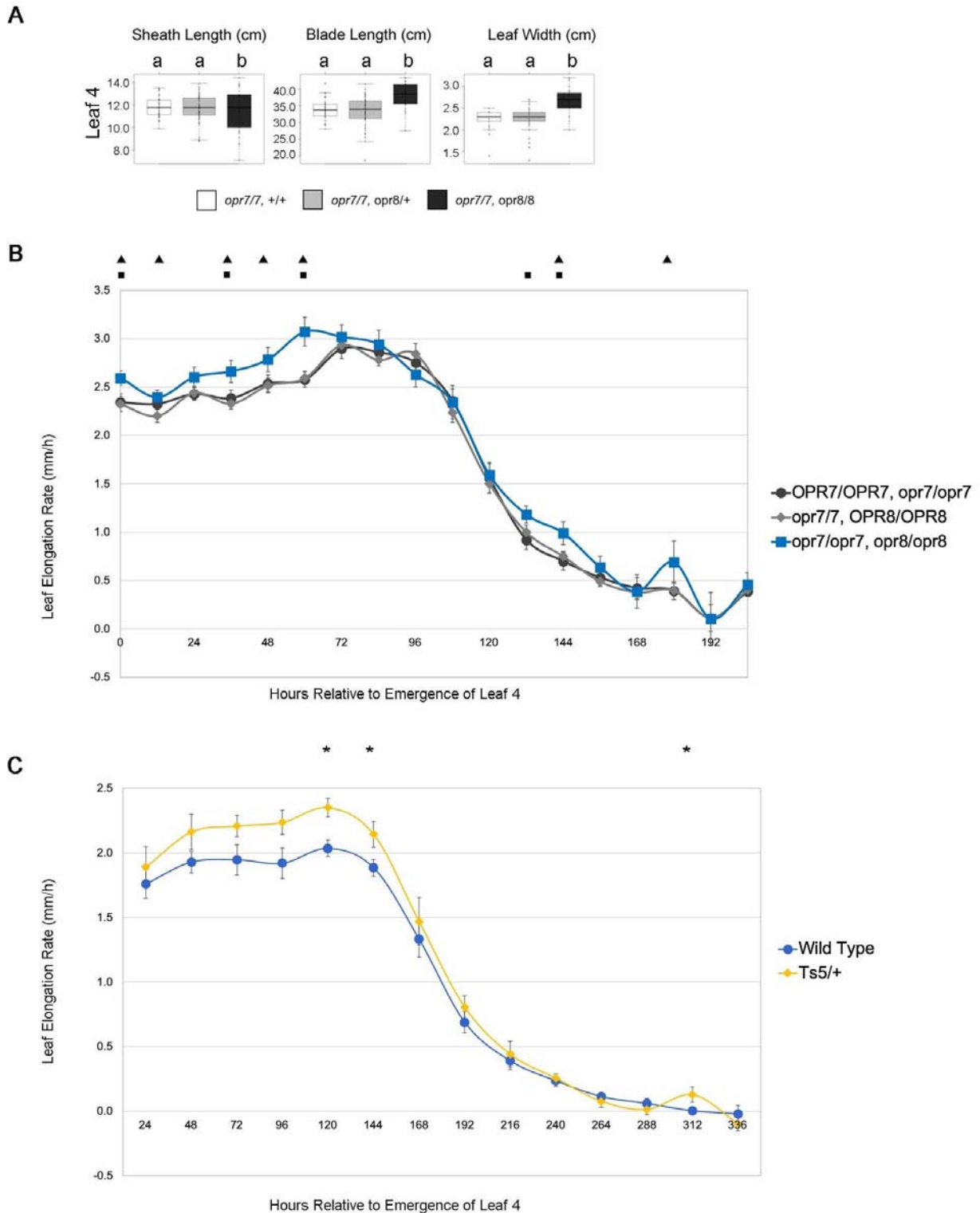
696

697 **Figure 4.** Final leaf size, leaf elongation rate (LER), and leaf elongation duration (LED) of
 698 *Hsf1*/⁺ and WT-siblings treated with 1 mM JA. Boxplots of leaves #3 **(A)** and #4 **(B)** of *Hsf1*/⁺
 699 and WT-siblings from seedlings grown from germinating seed subjected to a 6-day, 1 mM JA
 700 treatment. Horizontal bars represent the maximum, third quantile, median, first quantile, and
 701 minimum values respectively. Each dot is a plant (WT Control, n=7; WT JA, n=9; *Hsf1*/⁺ Control,
 702 n=10; *Hsf1*/⁺ JA, n=9). **(C-E)** LER superimposed over total leaf length. **(C)** LER and leaf lengths
 703 of WT and *Hsf1*/⁺ control treatments. JA treatment comparisons in **(D)** WT, **(E)** *Hsf1*/⁺, and **(F)**
 704 treated *Hsf1*/⁺ and WT. Significant differences by Student's t-test are marked by asterisks.

705 Yellow asterisks mark differences in LER and black asterisks mark differences in leaf length.

706 Error bars = SE.

707

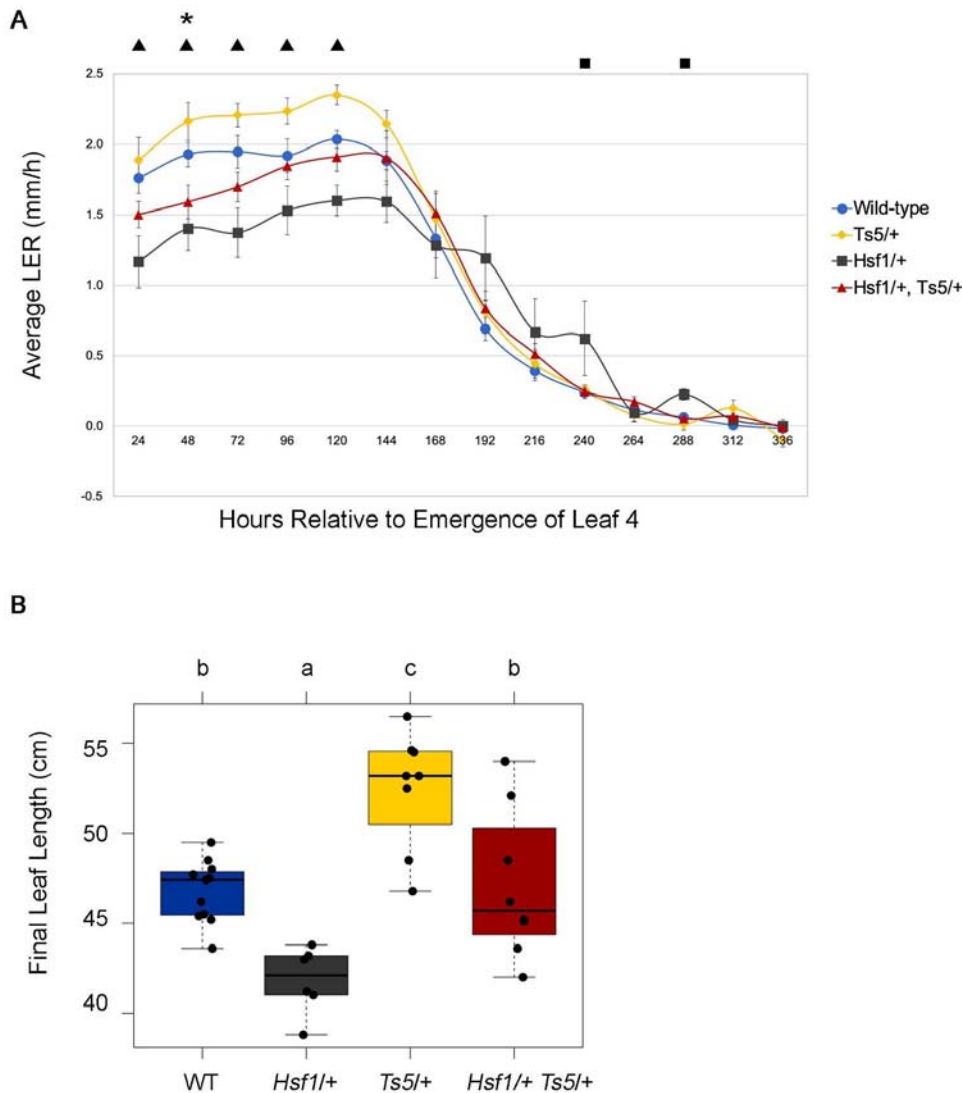


708

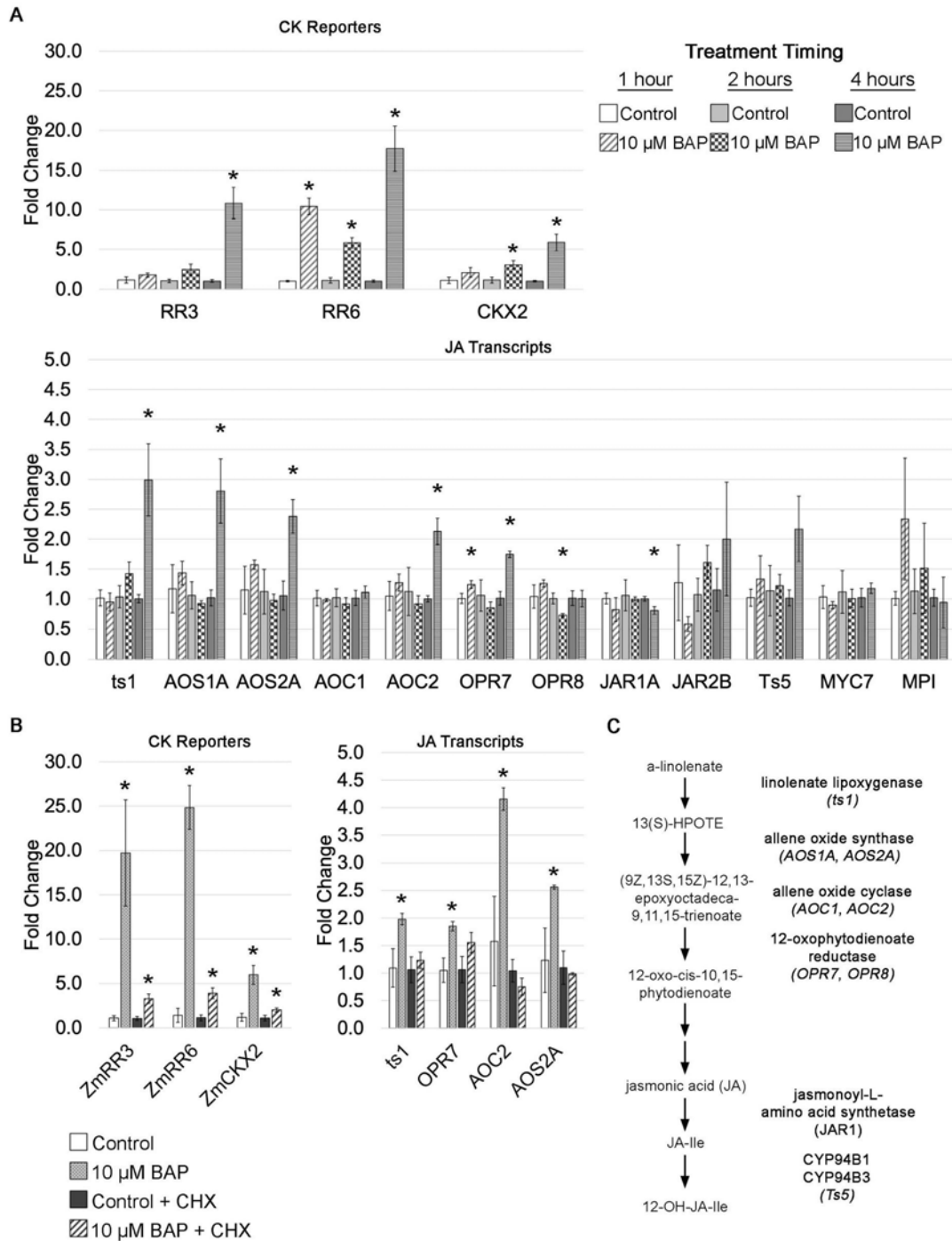
709 **Figure 5.** JA deficiency in maize enhances leaf growth. **(A)** Boxplots of sheath length, blade
 710 length, and blade width of the JA-deficient *opr7 opr8* double mutant as compared to its JA-
 711 sufficient siblings (*opr7/opr7, OPR8/OPR8* and *opr7/opr7, OPR8/opr8*). **(B)** LER of JA-deficient

712 *opr7 opr8* double mutant as compared to its JA-sufficient siblings *opr7/opr7*, *OPR8/OPR8* (black
713 triangles) and *opr7/opr7*, *OPR8/opr8* (black squares). Asterisks mark significant difference by
714 Student's t-test p-value ≤ 0.05 . Error bars = SE (*OPR8/OPR8*, n=34; *OPR8/opr8*, n=62;
715 *opr8/opr8*, n=33). **(C)** LER of JA-deficient *Ts5* dominant mutant compared to its JA-sufficient
716 WT-sibling. Asterisks mark significant difference $P < 0.05$.
717

718



719 **Figure 6.** Epistatic interaction of *Hsf1* and *Ts5*. (A) LER of *Hsf1/+ Ts5/+* double mutant
 720 compared to WT (asterisk), *Hsf1/+* (black squares), and *Ts5/+* (black triangles). Black squares
 721 and triangles above the LERs mark significant difference by Student's t-test p-value ≤ 0.05 .
 722 Error bars = SE (+/+, n=12; *Hsf1/+*, n=6; *Ts5/+*, n=9, *Hsf1/+ Ts5/+*, n=10). (B) Boxplots of
 723 sheath length, blade length, and blade width of leaf #1 and #2 of the population described in (A).
 724 Horizontal bars represent the maximum, third quantile, median, first quantile, and minimum
 725 values respectively. Each dot is a plant.
 726



728

729

730 **Figure 7.** CK induces JA pathway gene expression in the leaf growth zone. **(A)** Quantitative
 731 Real-time PCR analysis of CK reporter genes and JA biosynthesis and signaling genes after 10
 732 μM BAP time course. **(B)** Quantitative Real-time PCR analysis of CK reporter genes and JA
 733 biosynthesis genes after 10 μM BAP with and without cycloheximide (CHX) treatment. **(C)**

734 Synopsis of JA pathway genes surveyed in (A) and (B). Asterisks in (B) and (C) mark significant
735 difference ($P < 0.05$) between treatment and respective control.

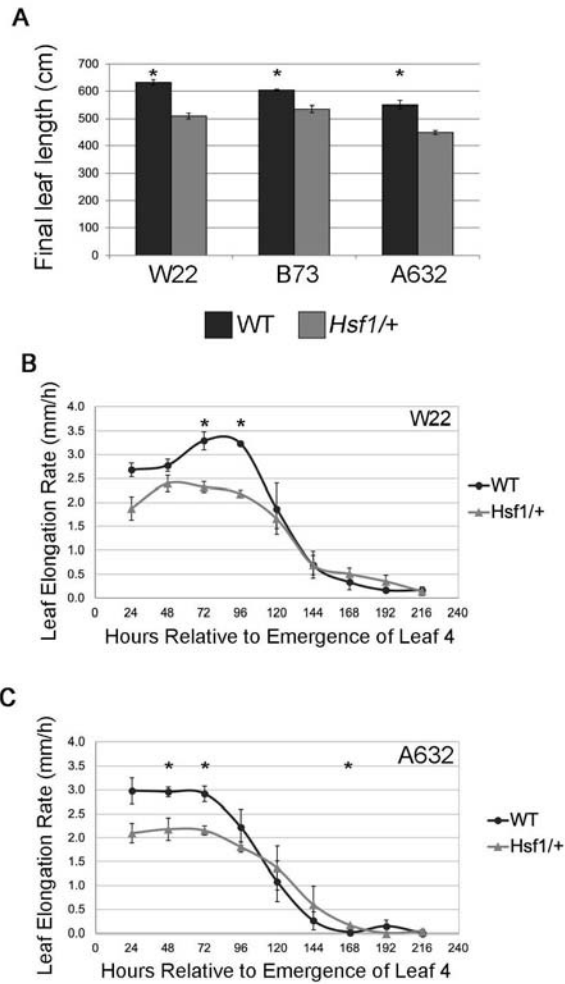
736

737

738

739 **SUPPLEMENTAL DATA**

740



741

742

743 **Supplementary Figure S1. *Hsf1* growth in different inbred backgrounds. (A)** Barplots of

744 WT and *Hsf1/+* final leaf lengths. Error bars = SE. **(B-C)** Average leaf elongation rate (LER) of

745 leaf #4 of *Hsf1/+* and WT-siblings in the **(B)** W22, and **(C)** A632 inbred backgrounds. Asterisks

746 mark significant difference $P < 0.05$. Error bars = SE.

747 **Supplemental Table S1.** Percent leaf size reduction after exogenous 1 mM JA
748 treatment. Percent reductions $[(JA-C)/C * 100]$ in sheath length, blade length, and blade
749 width by leaf number. Red means significant value $P < 0.05$.

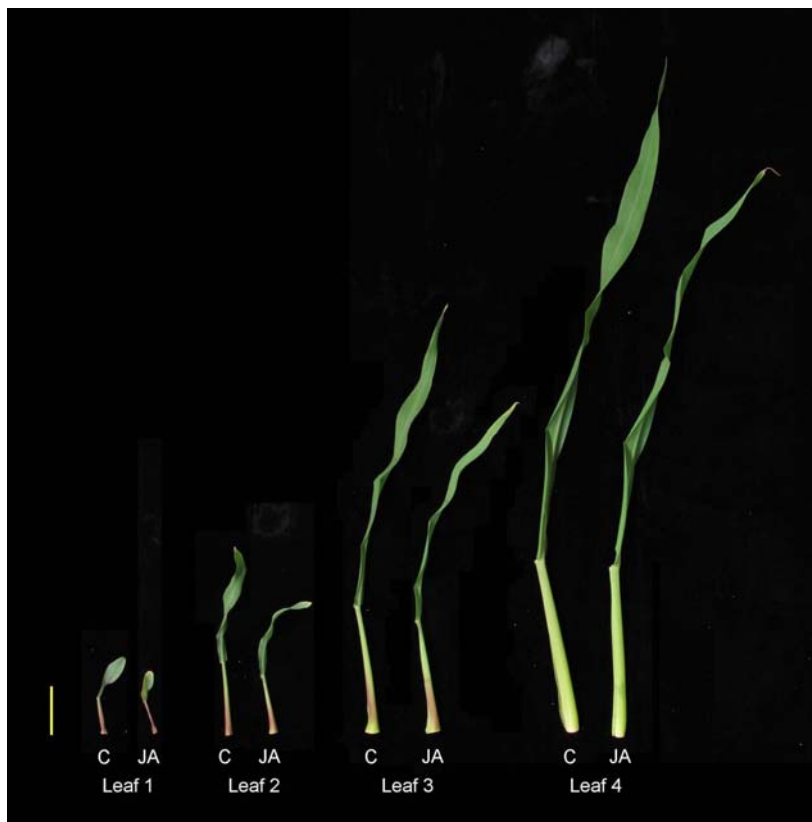
750

	Leaf 1	Leaf 2	Leaf 3	Leaf 4
Sheath Length	-23.30%	-30.90%	-21.90%	-17.80%
Blade Length	-29.90%	-28.70%	-30.50%	-26.00%
Blade Width	-18.70%	-9.30%	-15.30%	-14.30%

751

752

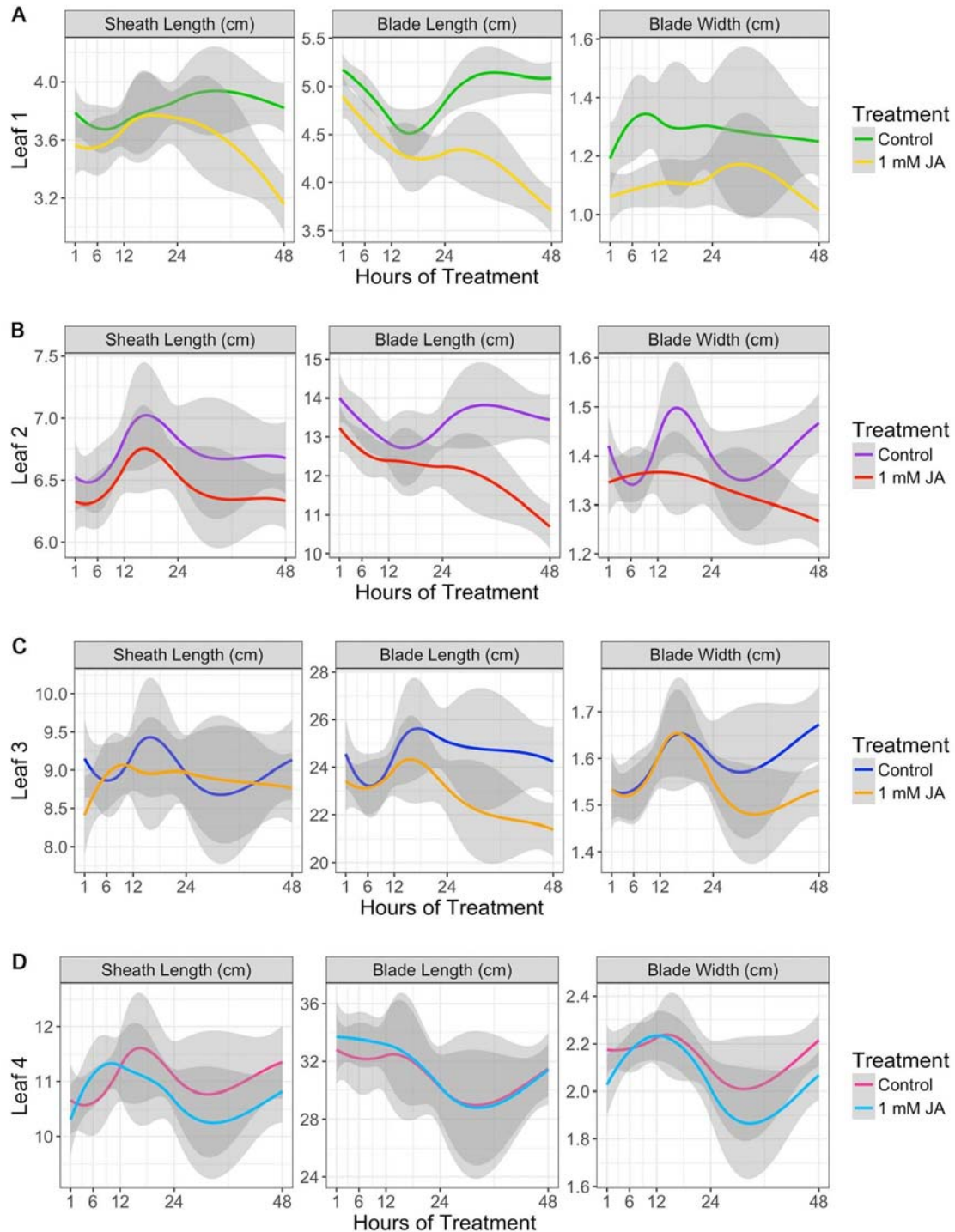
753



754

755 **Supplementary Figure S2.** Comparison of control (C) and jasmonic acid (JA) treated
756 leaves #1-4. Scale bar = 5 cm.

757



758

759 **Supplemental Figure S3.** Final leaf measurements of B73 treated with 1 mM JA or control
760 solution for 1, 6, 12, 24, or 48 hours. Leaf 1 (A), leaf 2 (B), leaf 3 (C), and leaf 4 (D) were
761 measured for all plants. Each dot is plant, lines are smoothed conditional means, and shaded

762 area is the 95% confidence interval. Treatments are significant where confidence intervals do
763 not overlap.

764

765 **Supplemental Table S2.** Percent leaf size reduction after 48 hours of exogenous 1 mM JA
766 treatment. Percent reductions [(JA-C)/C *100] in sheath length, blade length, and blade width by
767 leaf number. Red means significant value $P < 0.05$.

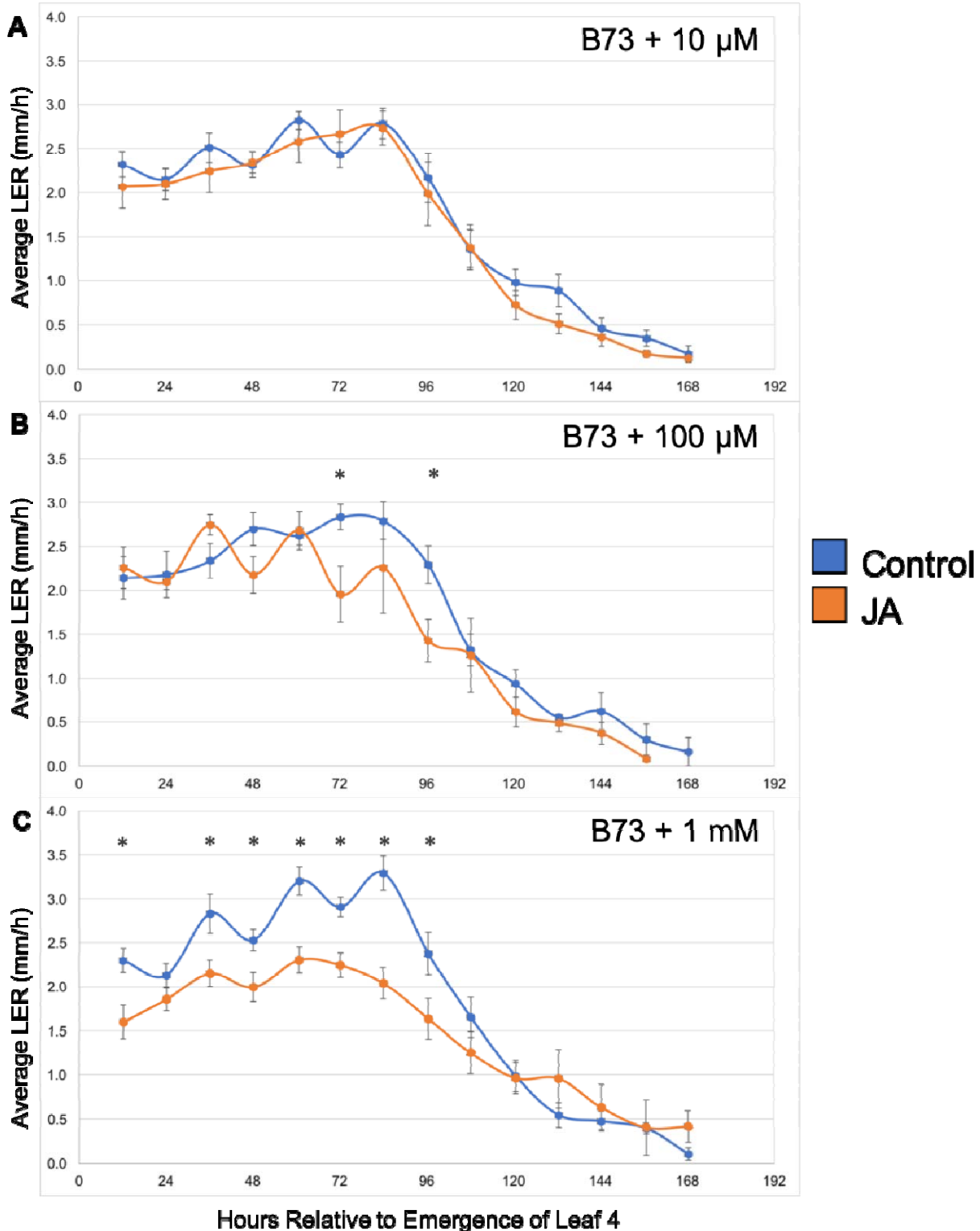
768

	Leaf 1	Leaf 2	Leaf 3	Leaf 4
Sheath Length	-17.30%	-5.20%	-4.00%	-4.70%
Blade Length	-27.10%	-20.50%	-11.70%	-0.30%
Blade Width	-18.80%	-13.60%	-8.50%	-6.70%

769

770

771



772

773 **Supplemental Figure S4.** LER dose response to JA in B73. Leaf 4 LERs of B73 treated with
774 (A) 10 μ M, (B) 100 μ M, and (C) 1 mM JA for 6 days. Significant differences by Student's t-test
775 are marked by asterisks and error bars are SE.

776 **Supplemental Table S3.** Relevant comparisons of *Hsf1/+* and WT-sibling final leaf size percent
 777 reductions after JA treatment. (i) WT-sibling compared to *Hsf1/+* without JA, (ii) WT-sibling with
 778 JA treatment, (iii) *Hsf1/+* with JA treatment, (iv) WT-sibling compared to *Hsf1/+* both treated with
 779 JA. Red means significant percent difference $P < 0.05$.

780
 781

i. WT Control vs. <i>Hsf1/+</i> Control				
	Leaf 1	Leaf 2	Leaf 3	Leaf 4
Sheath Length	-22.20%	-18.40%	-16.50%	-14.50%
Blade Length	-20.20%	-21.90%	-22.80%	-13.50%
Blade Width	-22.90%	-20.60%	-21.80%	-15.20%
ii. WT Control vs. WT JA				
	Leaf 1	Leaf 2	Leaf 3	Leaf 4
Sheath Length	-28.80%	-16.90%	-15.90%	-12.20%
Blade Length	-44.80%	-39.00%	-25.80%	-18.90%
Blade Width	-27.80%	-23.40%	-20.40%	-10.60%
iii. <i>Hsf1/+</i> Control vs. <i>Hsf1/+</i> JA				
	Leaf 1	Leaf 2	Leaf 3	Leaf 4
Sheath Length	-16.50%	-15.80%	-15.00%	-7.80%
Blade Length	-38.10%	-37.40%	-25.30%	-17.50%
Blade Width	-29.00%	-9.20%	-17.60%	-13.40%
iv. WT JA vs. <i>Hsf1/+</i> JA				
	Leaf 1	Leaf 2	Leaf 3	Leaf 4
Sheath Length	-8.80%	-17.30%	-15.60%	-10.20%

Blade Length	-10.50%	-19.80%	-22.40%	-12.00%
Blade Width	-24.20%	-5.90%	-19.10%	-17.90%

782

783

784 **Supplemental Table S4.** Relevant comparisons of *opr7 opr8* double mutant final leaf size
785 percent reductions. (i) *opr7 opr8* compared to JA sufficient *opr7/opr7 OPR8/opr8* (ii) *opr7 opr8*
786 compared to JA sufficient *opr7/opr7 OPR8/OPR8*. Red means significant percent difference $P <$
787 0.05.
788
789

i. <i>opr7/opr7 opr8/opr8</i> vs. <i>opr7/opr7 OPR8/opr8</i>				
	Leaf 1	Leaf 2	Leaf 3	Leaf 4
Sheath Length	39.5%	22.2%	11.0%	-1.4%
Blade Length	43.0%	36.8%	22.6%	14.2%
Blade Width	-7.6%	-1.6%	10.0%	17.6%
ii. <i>opr7/opr7 opr8/opr8</i> vs. <i>opr7/opr7 OPR8/OPR8</i>				
	Leaf 1	Leaf 2	Leaf 3	Leaf 4
Sheath Length	43.3%	21.0%	12.4%	-2.3%
Blade Length	48.2%	38.2%	24.2%	12.9%
Blade Width	-9.5%	-4.8%	9.2%	18.6%

790
791

792 **Supplemental Table S5.** The list of primers used in this study.

793

Primer Name	Target Gene (MaizeGDBloci)	Sequence (5'[Symbol]3')	Product(bp)	Purpose
ARV0090*	Mu-9242	AGAGAAGCCAACGCCAWCGCCTC YATTTTCGTC	varies	Genotype <i>opr7</i> <i>opr8</i>
ARV0097	<i>OPR7</i> (Zm00001d032049)	CGACACACATGCTCAAATCGAGA	WT = 816	
ARV0098		CTCCACCAGACCATCAGATCTAGC	Mu = 418/398	
ARV0099	<i>OPR8</i> (Zm00001d050107)	TATGGCAAGTATCCA ACTCCGAG G	WT =942	
ARV0100		ACACGAACAATAGTCCGCCTCTTA	Mu =530/412	
ARV0143	<i>Ts5</i> (Zm00001d049201)	ACACGCAATGTTTTTGCTGC	WT = 129	
ARV0144		ggccgtatcttcgctggata	Ts5/+ = 129/138	
ARV0129	<i>abphy1</i> (Zm00001d002982)	AGGATTTCTCTGCTGAAGC		qRT-PCR
ARV0130		GACACAGAGCTTCGGAAT		
ARV0131	rr6	TCATGTCATCGGAGAACGTG		qRT-PCR
ARV0132		TCCCCCAAATGTTAGCTC		
ARV0113	<i>CKO2</i> (Zm00001d042148)	TTCAACCCTCCTTCCGTCTTCC	135	qRT-PCR
ARV0114		TGGGGAGCTTGGAATCAGAAG G		
ARV0177	<i>ts1</i> (Zm00001d003533)	CCCCAACAGCGTTACCATTT	191	qRT-PCR
ARV0178		CTGTTCCGACCACCAAATCA		
	aos1a			qRT-PCR
	aos2a			qRT-PCR
	aoc1			qRT-PCR
	aoc2			qRT-PCR

	opr7			qRT-PCR
	opr8			qRT-PCR
	jar1b			qRT-PCR
	jar2b			qRT-PCR
	ts5			qRT-PCR
	myc7			qRT-PCR
	mpi			qRT-PCR

794 *Serves as a forward and reverse.